Quart. J. R. Met. Soc. (1978), **104**, 189–199

551.515.31

Tornadogenesis

By R. K. SMITH and L. M. LESLIE

Department of Mathematics, Monash University Clayton, Australia 3168

Australian Numerical Meteorology Research Centre, P.O. Box 5089AA, Melbourne, Australia 3001

(Received 18 February 1977; revised 1 June 1977

Summary

In this paper we use a simple numerical model to study vortex growth in a flow configuration which broadly simulates the principal characteristics of a severe tornadic storm system, i.e. strong vertical forcing by intense cumulus or cumulonimbus convection in the presence of an organized field of rotation on the cloud scale. The model is similar to one described by L. M. Leslie in which the updraught in the main cloud cell is modelled by an imposed body force, but differs in that the rotation field is determined by specifying the vertical profile of swirling velocity at the lateral boundary of the flow domain and air is allowed to enter or leave the computational region through its radial and upper boundaries. In particular, we compare situations in which the imposed swirl is concentrated aloft, primarily above cloud base, and when it extends to lower levels. In the former case, solutions exhibit genesis to a steady suspended vortex provided that the forcing strength lies within a certain range, depending on the level of rotation. However, if the imposed swirl extends sufficiently far below cloud base, the vortex continues its downward growth and establishes contact with the ground.

We believe our results provide a plausible and consistent picture of the growth of a tornado beneath the main updraught of a severe thunderstorm and indicate why only a relatively small proportion of such clouds spawn pendant funnel clouds and why only a fraction of these develop into tornadoes. Moreover, they appear to be consistent with the observed development of circulation patterns deduced from single-pulse Doppler radar measurements of a tornado-producing storm system by Burgess, Lemon and Brown.

1. Introduction

Owing to their extreme violence and capricious nature, and also their relatively short lifetime, small scale and comparative rarity, tornadoes have so far defied systematic attempts to probe their dynamics. Much of our knowledge is based on circumstantial evidence: for example, attempts have been made to deduce velocity fields from damage patterns and from the motion of debris caught up in the vortex, whilst maximum-wind estimates have been based also on the severity of damage. Information of this type, which is necessarily of low quality, is supplemented by laboratory and numerical vortex studies and by scale analyses of the equations of motion. However, there is still uncertainty about quite fundamental aspects, such as the pattern of motion parallel to the tornado axis, and one can only conjecture on the structure of the vortex above cloud base. It is also not known for certain what triggers a tornado since thunderstorms which are apparently suitable only occasionally spawn a vortex, but such information is vital if improved warnings are to become possible. This especially important problem is one which provides the central motivation for our paper.

As a preliminary step towards understanding tornadogenesis we must identify a mesoscale source of enhanced ambient rotation, strong enough to explain the observed circulation of a tornado, together with a driving mechanism strong enough to initiate and maintain a considerable local amplification of the rotation.

There seems little doubt that a tornado is driven by intense convection within the parent cloud system as it is difficult to conceive another mechanism capable of maintaining the huge pressure reduction across the vortex core. For intense vortices this has been estimated to be well in excess of 100 mb. It seems unlikely that buoyancy in the core

produced by latent heat release in the funnel cloud plays a dominant role in driving the vortex, otherwise one might expect to see some tornadoes without a parent cloud, or to see them forming prior to their parent cloud (see Morton 1966, p. 163).

The source of rotation is difficult to identify with as much certainty, at least in some cases. According to Davies-Jones and Kessler (1974), there appear to be two categories of tornadoes. The first type (we shall call them type A) form under new convective cells which continuously develop on the right rear flank of large cumulonimbus clouds and are thought to be triggered by the lifting of warm moist air, undercut by the cold downdraught of the cloud. The principal source of rotation for these tornadoes is by no means clear; there is undoubtedly enhanced cyclonic vorticity associated with the pseudo-cold-front of the downdraught, but whether or not there is an abundance of circulation above cloud base is not known. In some cases a vortex may form when the parent cloud top is only 4 km high, although rapid cloud development ensues. Type A tornadoes are generally the least severe type and are probably the counterpart of waterspouts which form under rapidly developing cumulus congestus clouds over the sea in warm sultry conditions. The downdraught frontal region of a neighbouring cloud has also been suggested as a possible source of rotation for a waterspout (Golden 1974, p. 102) but again there is uncertainty concerning the level and distribution of rotation pre-existing above cloud base.

The second type of tornado (which we shall call type B) is spawned beneath the updraught of a rotating cumulonimbus, sometimes called a 'tornado cyclone'. Unlike the more common cumulonimbi which are steered by the prevailing winds in mid-troposphere and have a multicellular structure, these storms move with a translation velocity component to the right (or occasionally to the left) of the mid-tropospheric winds and have an updraught in the form of a supercell (see, e.g., Browning 1968; Newton 1967). Typically, relatively dry air enters the storm at mid-levels ahead of the updraught, is cooled by precipitation falling into it and circles the updraught, at the same time descending to the rear of the storm to form an extensive downdraught. The storm propagates as the downdraught progressively undercuts warm moist air, which enters the storm at low levels on the forward right flank, ascends in an intense updraught and flows out ahead of the storm in the upper troposphere (see Browning Fig. 2(b), p. 431). It is thought that the shearing region separating the updraught from the mid-level inflow as the latter passes around the updraught and descends, provides a suitable source of vertically orientated, cyclonic vorticity for tornadogenesis.

Having identified a driving mechanism and a likely source of rotation, we are led to explore ways in which the rotation may be organized to form a concentrated vortex. The possibility of generating vortices from above in a rotation-rich environment has been demonstrated in laboratory experiments by Turner (1966), Ying and Chang (1970) and Ward (1972). In Turner's experiments, a vortex is produced in a cylindrical container of water, rotating with its axis vertical, by releasing a continuous stream of bubbles from a fine tube along the upper part of the axis. As the bubbles rise, they exert a drag on neighbouring fluid and thereby induce a meridional circulation which leads to vortex formation provided that the bubbling rate is confined within an intermediate range of values for a given rotation rate. The process of vortex evolution from the moment bubbles are released has been elucidated by Leslie (1971) and Bode *et al.* (1975) in a numerical simulation of Turner's experiments. Immediately after the bubble supply is switched on, the local induced circulation causes fluid to be drawn radially inwards towards the lower end of the bubble stream. Since angular momentum is conserved, a ring of converging fluid acquires increasing cyclonic relative rotation and continues inwards until there is a local balance between the centrifugal force and the radial pressure gradient; if the bubbling rate is too strong, balance is never achieved and if it is too weak, balance is reached after

only a small radial displacement; in neither case does a concentrated vortex form. At levels where cyclostrophic balance is established, further radial entrainment is inhibited, and free or relatively free radial entrainment is possible only at successively smaller and smaller heights. Thus the vortex extends progressively downwards until it begins to interact with the lower boundary. There it forms an inflow boundary layer in which cyclostrophic balance is no longer possible owing to friction, leaving a net, radially-inwards pressure gradient.

This mechanism of vortex growth provides an appealing explanation for the genesis of type A tornadoes, assuming that the downdraught frontal region provides an adequate source of low-level rotation and that rapid cumulus development induces convergence analogous to the bubbles. Indeed, the downward growth is consistent with the observed development of tornadoes, and the requirement that the driving force be confined within certain limits for given rotation strength suggests why only a fraction of apparently suitable storms actually spawn a tornado. It is less obvious that the mechanism extends to explain the growth of type B tornadoes as the source of rotation for these appears to be concentrated primarily within the cloud, at least in the early stages of growth, whereas the foregoing arguments assume that at every level above the friction layer, fluid entrained into the lower end of the developing vortex has sufficient angular momentum to attain cyclostrophic balance at an inner radius. This may not be the case if there is little ambient rotation at low levels.

It is also conspicuous that in all the laboratory and numerical simulations to date, there is an adequate supply of low-level rotation and that all the vortices produced extend to the lower boundary. In nature, however, not all vortices spawned from convective clouds establish contact with the ground and only a fraction of suspended vortices, seen in the form of pendant funnel clouds below the parent clouds, develop into tornadoes. There appear to be a number of possible explanations for this: for example, it may be that the convection and/or the rotation is not always sustained for long enough, or with sufficient strength, to permit downward extension of the vortex to the ground. On the other hand, the vortex may extend to the ground but may be too weak to produce either a complete visible funnel or a significant disturbance at ground level: this is sometimes true in the case of waterspouts which proceed little further than the 'dark spot' stage; see Golden (1974). A further possibility is discussed in section 4.

In this paper we describe a numerical model which demonstrates the possibility of downward vortex growth in a flow configuration where the ambient rotation and the driving mechanism are concentrated aloft. The model also demonstrates the possibility of maintaining steady suspended vortices under certain circumstances.

2. The model

The flow domain over which computations are performed is a cylindrical region of air with radius R and depth H with its axis vertical (Fig. 1(a)). It is bounded by a rigid (no-slip) lower boundary and has a porous side wall and upper boundary through which air may enter or leave the cylinder in a normal direction (in one experiment, only the upper portion of the side wall is porous: see below). The flow is taken to be axisymmetric and is driven by a body force imposed along the upper part of the axis; this force may be thought of as a crude but simple representation of a convective cloud updraught. Rotation is imposed by prescribing a swirling velocity component on fluid entering through the porous part of the side wall, or a portion of it. Furthermore, the air is taken to be homogeneous and incompressible with density ρ and turbulent diffusivity of momentum K_M, assumed to be constant.

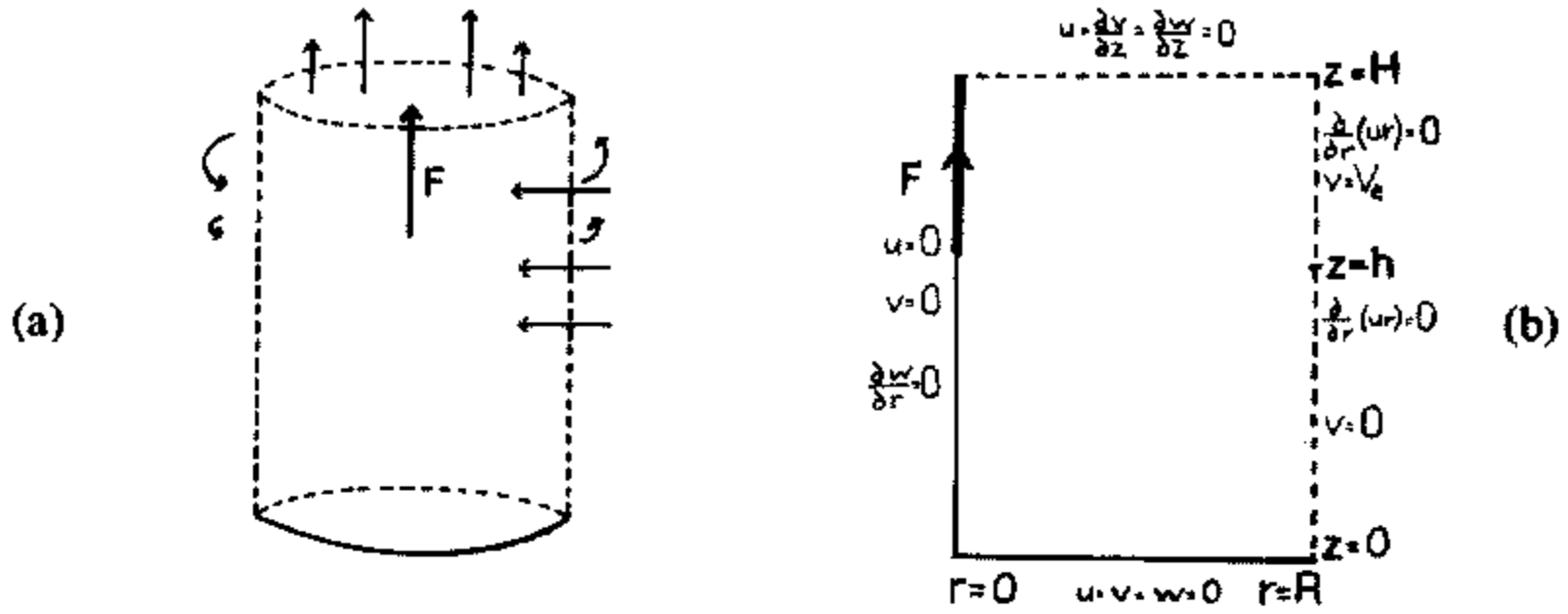

Figure 1. (a) Schematic diagram of the flow configuration under study. (b) Boundary conditions for this flow.

In spite of its simplicity, this flow contains the two most basic features of a type B tornado system: a source of rotation and a driving mechanism, both concentrated aloft.

The equations of motion and continuity are $D\mathbf{u}/Dt = -(1/\rho)\nabla p + F\mathbf{k} + K_M\nabla^2\mathbf{u}$ and $\nabla.\mathbf{u} = 0$, where $\mathbf{u}, = (u, v, w)$, is the velocity referred to a cylindrical coordinate system (r, θ, z), coaxial with the computational region; p is the dynamic pressure; F is the body force per unit mass; $\mathbf{k}$ is the unit vector $(0, 0, 1)$; and t measures time.

The boundary conditions conforming with the model description given above are displayed in Fig. 1(b); they are as follows:

On $z = 0$: $u = 0, v = 0, w = 0,$
On $z = H$: $u = 0, \partial v/\partial z = 0, \partial w/\partial z = 0,$
On $r = 0$: $u = 0, v = 0, \partial w/\partial r = 0,$
On $r = R$: $\partial(ur)/\partial r = 0, v = V_e$ (a constant) for $h < z < H,$
$v = 0$ for $0 \leqslant z < h, w = 0.$

These conditions are not all independent. In one experiment the lower portion of the side wall is rigid so that the modified boundary condition on $r = R$ becomes $u = 0$, $v = 0$, $w = 0$, for $0 \leqslant z < h < H$.

The numerical method is essentially the same as that used by Bode *et al.* (1975) and the details are not repeated here. Briefly, the equations of motion and boundary conditions are expressed in a form suitable for numerical integration and the calculations are commenced from an initially quiescent state $\mathbf{u} \equiv 0$, with the body force applied impulsively at the initial instant, $t = 0$. The integrations are carried out until a steady state is attained and the flow fields presented later all relate to this state. The finite difference mesh has 101 points in the vertical and 67 in the horizontal in each experiment. The calculations were performed on the CSIRO, Cyber 76 computer in Canberra.

3. Parameter values

Although we have not set out to model a tornado and its parent cloud directly in our experiments, we have chosen, where possible, parameter values broadly appropriate to the atmospheric situation. Thus, in the three experiments for which we present results, the parameters in common have values: $R = 2\,\text{km}$, $H = 3\,\text{km}$, $V_e = 2{\cdot}5\,\text{m s}^{-1}$ (corresponding with a circulation $\Gamma, = 2\pi RV_e$, equal to $3{\cdot}1 \times 10^4\text{m}^2\text{s}^{-1}$ and a mean vertical vorticity, $\Gamma/\pi R^2$, equal to $2{\cdot}5 \times 10^{-3}\text{s}^{-1}$), $\rho = 1{\cdot}2\,\text{kg m}^{-3}$ and $K_M = 10\,\text{m}^2\text{s}^{-1}$. Rather than attempt to use cloud buoyancy data to obtain a suitable magnitude for F, we have determined by trial and error a value which leads to a strong concentrated vortex for the imposed circulation, Γ (as noted earlier, concentrated vortices will form only for a restricted range of F for a given circulation: see the appendix and, e.g., Morton 1969). Accordingly, we take the body force to have a maximum value of $2{\cdot}4\,\text{m s}^{-2}$ on the axis, tapering linearly to zero

at two grid lengths from the axis, and to have its lower end at a height of 1·5 km, which we shall refer to loosely as the 'cloud base' (for additional comment on this choice, see section 5).

4. Experimental results

The four experiments described in detail below differ only in their side boundary conditions. In experiment 1, air may enter the side boundary only above 'cloud base' and as it does so it acquires cyclonic rotation; below this level the boundary is rigid. In experiments 2, 3 and 4, air may enter or leave through the entire side boundary but only that which enters above a height h ($< H$) acquires rotation (strictly, the imposed swirling velocity at $r = R$ is reduced linearly from its uniform value V_e at one grid spacing above $z = h$ to zero at one grid spacing below $z = h$). In experiment 2, the imposed circulation is confined above cloud base ($h = 1{\cdot}5$ km) whereas in experiment 3, there is an extensive region of circulation below cloud base ($h = 0{\cdot}75$ km) and in experiment 4, the region of circulation extends to the ground ($h = 0$). Clearly, with its rigid side boundary, experiment 1 is not at all relevant to the atmosphere but it provides a convenient starting point for the development of our ideas and allows informative comparisons to be made with the other experiments.

The streamlines for the mature flow fields in experiments 1, 2 and 3 are shown in Fig. 2 and the corresponding isotachs of swirling velocity and isobars of dynamic pressure are shown in Figs. 3 and 4 respectively. Additional data derived from the four calculations are listed in Table 1: this includes the maximum vertical velocity, w_{max}; the maximum swirling velocity, v_{max}, together with the radius r_{max} at which this occurs; the maximum pressure

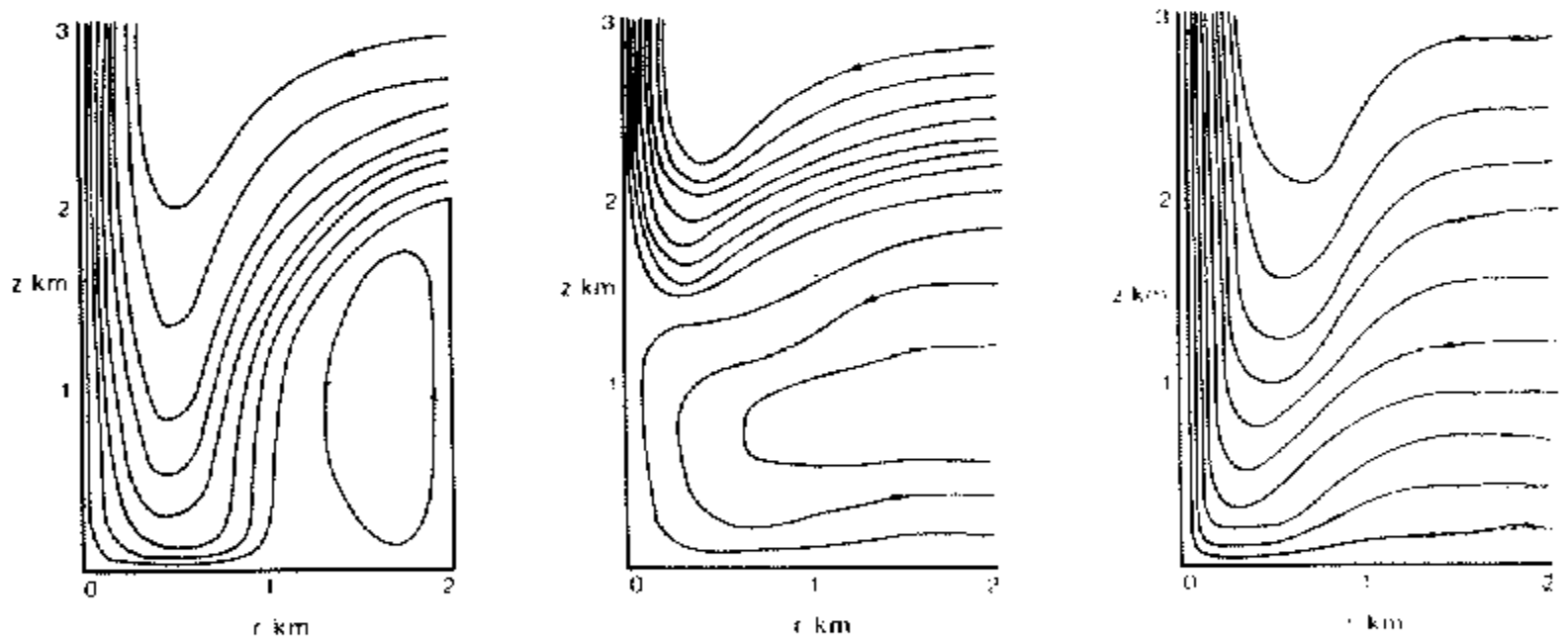

Figure 2. Streamlines for the meridional flow in experiments 1, 2 and 3, labelled (a), (b) and (c) respectively. Note: these are intended to give an indication of the flow patterns only and the contours are not everywhere equi-spaced.

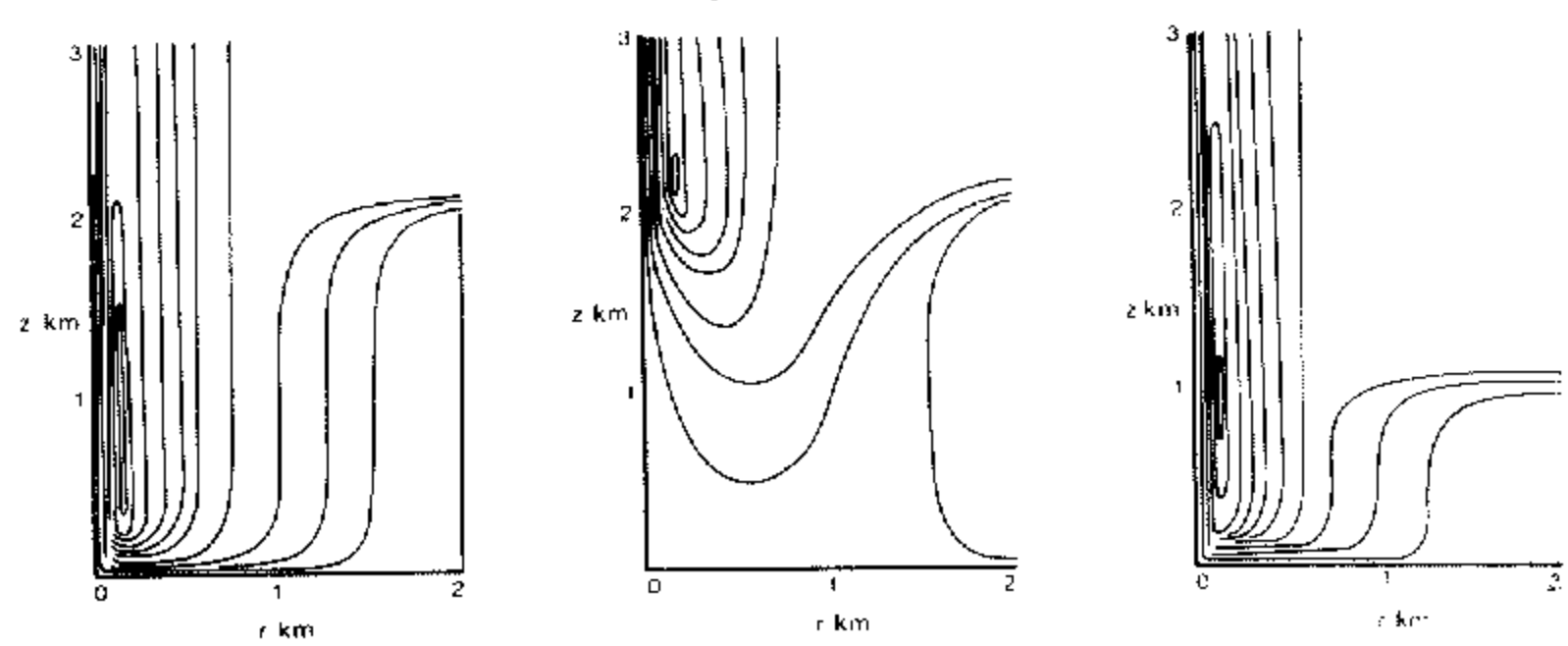

Figure 3. Isotachs of swirling velocity; otherwise as in Fig. 2.

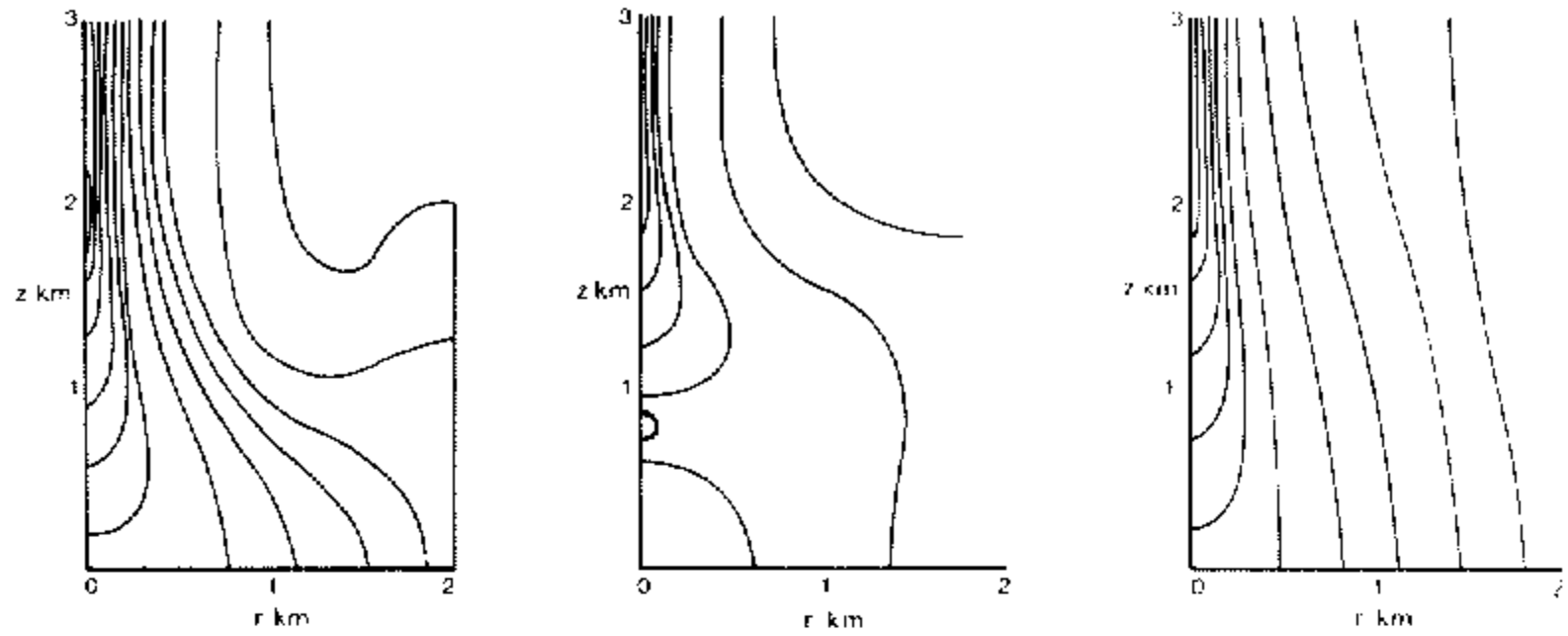

Figure 4. Isobars of dynamic pressure; otherwise as in Fig. 2.

reduction across the vortex, Δp; the time taken to reach the steady state, T_F (based on the arbitrary criterion that the total kinetic energy changes by less than one percent over ten time steps) and the'amplification factor', A, defined as $(v_{max}/r_{max})/(V_e/R)$, a measure of the angular rotation of the vortex core compared with that of the ambient field of rotation.

TABLE 1. DERIVED VORTEX CHARACTERISTICS FOR THE FOUR PRINCIPAL NUMERICAL EXPERIMENTS

	Experiment 1	Experiment 2	Experiment 3	Experiment 4
$w_{max}(m\,s^{-1})$	71	53	62	77
$v_{max}(m\,s^{-1})$	64	52	57	70
$r_{max}(m)$	40	47	43	38
Δp (mb)	52	32	46	59
T_F(min)	4½	3¼	4¼	4½
A	1290	890	1050	1470

In experiment 1, the vortex grows down to the lower boundary by the mechanism explained in section 1. This is possible because all the air which is entrained into the lower end of the developing vortex enters through the side boundary, where it acquires sufficient angular momentum to reach cyclostrophic balance at some inner radius (presumably this argument holds only so long as the main body of flow is dominated by advection; if, for example, H is increased, keeping $H-h$ and all other parameters fixed, one anticipates that a stage will be reached where the inflow towards the end of the developing vortex is controlled by viscous effects rather than by the cyclostrophic constraint).

In experiment 2, air may cross the side boundary below cloud base (a situation which obviously models the atmosphere more closely) but the circulation at this boundary is still held zero at these levels. During the early stages of growth, the incipient vortex draws predominantly on air which enters the side boundary above cloud base; as in experiment 1, this air carries angular momentum with it and the vortex descends. However, as it grows down it begins to draw on air originating through the side boundary at levels where there is no imposed rotation and the downwards growth terminates aloft. In the mature state, a little of this air enters the vortex core through its lower end but most of it circulates as shown in Fig. 2(b) and diverges at low levels. In this configuration, therefore, a steady, suspended vortex is maintained. Perhaps not surprisingly, this vortex is weaker and slightly broader than that obtained in experiment 1 (see Table 1). It is also important to note that further downward extension of the vortex cannot be predisposed merely by increasing the forcing strength as this simply augments the entrainment of non-rotating air from lower levels; indeed a calculation of this kind in which the forcing strength was doubled produced a much weaker and broader vortex with $v_{max} = 36\,m\,s^{-1}$, $r_{max} = 60\,m$ and $A = 480$.

It is now of interest to compare experiment 2 with experiment 3 in which air entering through the side boundary down to a height of 0·75 km has rotation. In this case, the vortex

extends to the lower boundary (Figs. 2(c) and 3(c)) and there is no low-level meridional circulation with divergence near the ground. The mature vortex is again weaker than that in experiment 1, especially just above the ground, since air which enters the vortex at low levels originates through the lowest part of the side boundary (Fig. 3(c)) where there is no imposed rotation. This air acquires angular momentum only by diffusion from the flow above. The inflow boundary layer adjacent to the ground is likewise less pronounced than in experiment 1 (compare Figs. 1(a) and 1(c)) in accordance with the weaker swirl, and this is reflected in the smaller maximum vertical velocity – see Table 1.

In experiment 4, where the rotation is imposed over the whole side boundary, the flow patterns (not shown) are similar to those in experiment 3 but the vortex is now much stronger, even than that in experiment 1, and there is a strong inflow boundary layer. Data for this calculation are included in Table 1.

Finally, we note that the dynamic pressure fields shown in Fig. 4 are consistent with the azimuthal and meridional circulations shown in Figs. 2 and 3. It is also interesting to note that the growth times of our simulated vortices are not unrealistic in relation to the observed development of tornadoes from cloud base to the ground and that the other flow quantities listed in Table 1 also lie within the ranges characteristic of these vortices.

5. Discussion

In the foregoing experiments we have demonstrated the possibility of downward vortex growth in a flow configuration where both the fields of rotation and the upward driving force are concentrated aloft. In this situation, the ambient rotational field develops downwards, with the vortex, due to the meridional circulation which the vortex induces. We have shown also that the vortex extends to the lower boundary only if the ambient rotation occurs at sufficiently low levels and that in other cases a steady, suspended vortex is maintained.

We believe the mechanism of growth we have described offers a plausible explanation for tornadogenesis, and it does not rely on submechanisms to trigger the vortex such as that suggested by Eskridge and Das (1976); see also Smith *et al.* (1977). Moreover, it gains considerable support from a series of high resolution, single pulse, Doppler radar observations of the 1973 Union City tornado reported by Burgess *et al.* (1975). In these observations, a vortex circulation on a scale only slightly larger than the radar resolution (~ 1 km), is revealed by radial velocity maxima of opposite signs between two radar range gates at adjacent azimuths; a situation referred to in the paper cited as gate-to-gate shear but recently renamed tornado vortex signature (TVS) by Burgess *et al.* (1976). From the data obtained, Burgess *et al.* (1975) draw the following tentative conclusions:

(i) the TVS extends well up into the storm and is contained within a parent circulation;

(ii) the larger circulation shrinks before tornado touchdown and the TVS migrates to the circulation centre;

(iii) the TVS is both definable and trackable for over 30 minutes prior to tornado touchdown; and

(iv) the TVS descends with time from the storm mid-levels to the surface and the surface TVS positions trace out the tornado track.

These inferences suggest strongly that the tornado is initiated from above by convergence of the existing cloud circulation in the manner we have described, and it is reasonable to assume that the convergence is associated with the large vertical acceleration within the cloud updraught.

The fact that a vortex can be generated in our experiments only when the forcing is confined within certain limits for a given strength of rotation would explain why only a few apparently suitable clouds spawn a vortex, since of the number of clouds having significant circulation, only a few would be expected also to have an updraught strength capable of concentrating the existing rotation to form a vortex. Our results also suggest that tornadogenesis requires a suitable spatial distribution of the rotation field and if the cloud circulation is confined predominantly to mid-levels, a pendant funnel cloud may develop but it may not evolve into a tornado.

We now consider certain aspects of the numerical model in detail in relation to tornadoes and their parent circulations. Firstly, we must expect some structural difference between our simulated vortices and tornadoes, for in at least a few cases, the latter show evidence of downflow in an axial core (not necessarily extending to the ground), and this feature has been confirmed in the case of waterspouts (Golden, p. 27). Indeed, axial downflow is likely to prevail in regions where a vortex suffers axial decay or radial spread (Morton 1969, p. 319; Smith and Leslie 1976, p. 797), but appears to be precluded in our model due to the location of the driving force along the axis. Presumably, with convective forcing, the lateral constraints on the buoyancy field are not so great and allow the latter to be organized so as to accommodate axial downflow, as in the case of dust devils (Smith and Leslie 1976). There is also a disparity between the lateral extent of the forcing in our model and in a cloud updraught and this is likely to be of some importance. In this connection, we note that the body force used in these calculations, and determined as described in section 3, corresponds with a mean buoyancy force per unit mass of 0·08 g. With a typical upper air temperature of 250 K, this corresponds with a temperature difference of 20K, which is too large by a factor of four or five, but the force is distributed over a radial extent of only 60 m. Further studies of these problems are planned and we hope to incorporate thermal forcing effects in a future model. Nevertheless, we do not believe the structural difference noted above invalidates the conclusions, nor detracts substantially from the relevance of our paper.

Our use of the term 'cloud base' for the height of the lower end of the forcing function is a useful aid to description but the analogy should not be interpreted too literally if, as we have tacitly assumed, the forcing field is taken to model the effect of buoyancy. Thus, in the case of a small cumulus cloud fed by a thermal from the subcloud layer, the forcing function would extend below cloud base. In contrast, the updraught in severe thunderstorms is frequently observed to be negatively buoyant in the lower part of the cloud and is therefore driven by dynamically induced pressure gradients at these levels (Marwitz 1973; Browning and Foote 1976, p. 506). In this situation, our 'forcing function' would refer to the buoyant part of the updraught in the middle and upper levels of the cloud.

The choice of swirling condition on the side boundary also merits further comment. In particular, in experiment 2 this condition may be improved by taking $\partial(rv)/\partial r\,|_{r=R} = 0$ wherever fluid leaves the computational region, thereby allowing angular momentum to be conserved on exit. However, since the low-level outflow rotates only weakly in experiment 2 (Fig. 3 (b)), we anticipate that this alternative condition would lead to only marginal differences in the flow obtained, although the differences might be more significant for some ranges of parameters. More generally, we consider briefly some implications of the prescription of swirling velocity (and hence circulation) at the side boundary, where an alternative condition might be to prescribe the vertical component of vorticity. A detailed comparison of these two boundary conditions is given in a recent paper by the authors (Leslie and Smith 1977) in the context of thermally driven vortices. It is shown that whereas the former condition corresponds approximately with an irrotational, ambient swirling flow at heights where diffusive effects are small, the latter approximates to the imposition

of ambient solid body rotation. Even so, the different conditions do not lead to dynamical differences between the vortices obtained. In the tornado situation, as in the dust devil case, neither boundary condition is likely to be strictly correct but for the limited objectives here, we believe the boundary condition chosen is adequate. Further studies of the problems involved in interfacing tornado models with models of the parent cloud-scale circulations are currently in progress, and the effects of stratification, which have been completely neglected here, are also being investigated.

Finally, we are aware of the limitations of using a constant turbulent diffusivity but in the absence of any guidance from observations, investigations of the effects of hypothetical variations in diffusivity are unlikely to be rewarding at the present time. However, we note that our previous vortex calculations show that the swirling flow field is relatively insensitive to the value of the diffusivity providing diffusive effects are not large (see Smith and Leslie, p. 802; Leslie and Smith, p. 509).

Acknowledgments

The first author is grateful to Drs Keith Browning, Bill Cotton and Martin Miller with whom he has had helpful discussions about this work and about severe storms in general. We are also grateful to Dr R. Davies-Jones of the National Severe Storms Laboratory for a number of constructive comments on the original version of the manuscript.

References

Bode, L., Leslie, L. M. and Smith, R. K. 1975 A numerical study of boundary effects on concentrated vortices with application to tornadoes and waterspouts, *Quart. J. R. Met. Soc.*, **101**, 313–324.

Browning, K. A. 1968 The organization of severe local storms, *Weather*, **23**, 429–434.

Browning, K. A. and Foote, G. B. 1976 Airflow and hail growth in supercell storms and some implications for hail suppression, *Quart. J. R. Met. Soc.*, **102**, 499–533.

Burgess, D. W., Lemon, L. R. and Brown, R. A. 1975 Evolution of a tornado signature and parent circulation as revealed by single doppler radar, *16th Radar Meteorology Conference*, Houston, Texas (American Meteor. Soc.), 99–105.

Burgess, D. W., Hennington, L. D., Doviak, R. J. and Ray, P. S. 1976 Multimoment Doppler display for severe storm identification, *J. Appl. Met.*, **15**, 1302–1306.

Davies-Jones, R. and Kessler, E. 1974 Tornadoes, in *Weather and climate modification*, Ed. W. N. Hess, John Wiley, 552–595.

Eskridge, R. E. and Das, P. 1976 Effect of a precipitation-driven downdraft on a rotating wind field: a possible trigger mechanism for tornadoes?, *J. Atmos. Sci.*, **33**, 70–84.

Golden, J. 1974 Life cycle of Florida Keys waterspouts, NOAA Technical Memo. ERL NSSL–70.

Leslie, L. M. 1971 The development of concentrated vortices: a numerical study, *J. Fluid Mech.*, **48**, 1–21.

Leslie, L. M. and Smith, R. K. 1977 On the choice of radial boundary conditions for numerical models of sub-synoptic vortex flows in the atmosphere with application to dust devils, *Quart. J. R. Met. Soc.*, **103**, 499–510.

Marwitz, J. D. 1973 Trajectories within the weak echo regions of hailstorms, *J. Appl. Met.*, **12**, 1174–1182.

Morton, B. R. 1966 Geophysical vortices, in *Prog. in Aeronautical Sci.*, **7**, 145–194 (ed. Küchemann) Pergamon.

1969 The strength of vortex and swirling core flows, *J. Fluid Mech.*, **38**, 315–333.

Newton, C. W. 1967 Severe convective storms, *Advan. Geophys.*, **12**, 257–308.

Smith, R. K. and Leslie, L. M. 1976 Thermally driven vortices: a numerical study with application to dust-devil dynamics, *Quart. J. R. Met. Soc.*, **102**, 791–804.

Smith, R. K., Mansbridge, J. V. and Leslie, L. M. 1977 Comments on 'Effect of a precipitation-driven downdraft on a rotating wind field: a possible trigger mechanism for tornadoes?', *J. Atmos. Sci.*, **34**, 548–549.

Turner, J. S. 1966 The constraints imposed on tornado-like vortices by the top and bottom boundary conditions, *J. Fluid Mech.*, **25**, 377–400.

Ward, N. B. 1972 The exploration of certain features of tornado dynamics using a laboratory model, *J. Atmos. Sci.*, **29**, 1194–1204.

Ying, S. J. and Chang, C. C. 1970 Exploratory model study of tornado-like vortex dynamics, *Ibid.*, **27**, 3–14.

Appendix

We have been unable to undertake a comprehensive study of parameter space for these models owing to computational expense, but to give some appreciation of the range of values of forcing strength for which a concentrated vortex forms, we have repeated experiment 4 with values of F on the axis, say F_0, equal to 0·6, 1·2, 3·6 and 4·8 m s^{-2}, keeping all other external parameters fixed and, in particular, the circulation maintained on the radial boundary. The vortex characteristics as F_0 changes are summarized in Fig. 5, which shows the variation of A, v_{max}, r_{max}, and w_{max} as functions of F_0. As F_0 increases from low values ($<0{\cdot}6$) to values between 3·0 and 4·0, A, v_{max} and w_{max} all increase, whereas r_{max} decreases. Thus, as the forcing strength becomes larger, fluid can be drawn in to smaller radii before local cyclostrophic balance is achieved and a stronger vortex results. As F_0

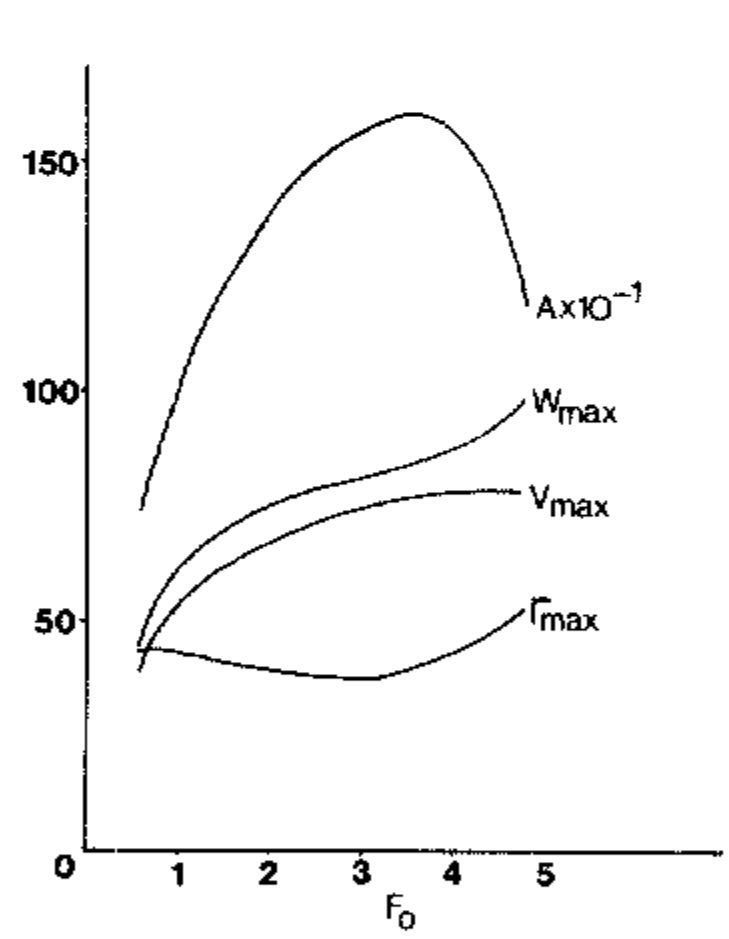

Figure 5. Variation of derived vortex characteristics as functions of F_0.

increases further, w_{max}, and hence the strength of the meridional circulation, continues to increase but the amplification factor decreases sharply, due mainly to the marked increase in r_{max} and to a lesser degree to the slight decrease in v_{max}. This is a reflection of the decreasing constraint of cyclostrophic balance as radial accelerations become significant throughout much of the flow. The sharpness of the peak of $A(F_0)$ is an indication of the extent to which the imposed circulation and forcing strength must be 'tuned' for a concentrated vortex to form. Finally, we note that the time taken for the flow to become established measured by T_F (see section 4) is relatively insensitive to the value of F_0 (the curve $T_F(F_0)$ is not shown).